

Nuclear Reactions Important in Alpha-Rich Freezeouts

George C. Jordan, IV, Sanjib S. Gupta, Bradley S. Meyer, Lih-Sin The^{1,*}

*¹Department of Physics and Astronomy,
Clemson University, Clemson, SC 29634-0978*

(Dated: November 4, 2018)

Abstract

The alpha-rich freezeout from equilibrium occurs during the core-collapse explosion of a massive star when the supernova shock wave passes through the Si-rich shell of the star. The nuclei are heated to high temperature and broken down into nucleons and α particles. These subsequently reassemble as the material expands and cools, thereby producing new heavy nuclei, including a number of important supernova observables. In this paper we introduce two web-based applications. The first displays the results of a reaction-rate sensitivity study of alpha-rich freezeout yields. The second allows the interested reader to run parameterized explosive silicon burning calculations in which the user inputs his own parameters. These tools are intended to aid in the identification of nuclear reaction rates important for experimental study. We then analyze several iron-group isotopes (^{59}Ni , ^{57}Co , ^{56}Co , and ^{55}Fe) in terms of their roles as observables and examine the reaction rates that are important in their production.

PACS numbers: 24.10.-i, 26.30.+k, 26.50.+x

*gjordan@clemson.edu; <http://photon.phys.clemson.edu/nucleo>

I. INTRODUCTION

Progress in the science of stars and their nucleosynthetic processes relies on the continued interplay of astronomical observations and astrophysical modeling. Observations of abundances of chemical species, elemental or isotopic, constrain astrophysical models while the models, in turn, provide a framework for interpreting the observations. It has long been clear, however, that uncertainties in the input physics to the models limit them and their usefulness in interpreting abundance observations. Nuclear reaction rates are key inputs into the astrophysical models, and, though many are measured, most have not, and modelers must therefore rely on theoretical predictions of the value of these rates. Recent theoretical reaction-rate predictions have proven fairly accurate (to within a factor of a few of the actual rate value where subsequently measured—e. g., [1]), nevertheless experimental results are usually desirable and often crucial. A third essential effort in nuclear astrophysics is that of nuclear experimentalists who seek to provide better input into astrophysical models by measuring the rates of nuclear reactions or nuclear properties that improve theoretical estimates of the rates. Because of the cost in time, effort, and financial resources in performing the necessary experiments, however, the task of the nuclear experimentalists is greatly aided if the astrophysical significance of a particular nuclear reaction can be clearly demonstrated. This in turn requires demonstration of the dependence of the predicted value of an astronomical observable in an astrophysical model on the value of the reaction rate. It is clear that observers, modelers, and experimentalists should all play an important role in the planning of nuclear astrophysics experiments, in particular by ensuring that any nuclear reaction rate proposed for experimental study satisfy the following four requirements [2]:

1. An appropriate astrophysical model of a nucleosynthesis process must exist.
2. An observable from that process, usually an abundance result, is either known or measurable.
3. The dependency of the value of the observable on the value of the nuclear cross section is demonstrable.
4. An experimental strategy for measuring the reaction rate, or at least using experimental data to better calculate the reaction rate, should be available.

A long-term goal of our program is to aid the dialogue among the three parties (observers, modelers, and experimentalists) in the nuclear astrophysics community by making it easier to identify those nuclear reactions most in need of experimental study. In the present work, we focus on reaction rates important in the alpha-rich freezeout in core-collapse supernovae. We explore in some detail astronomical observables from this process and the nuclear reactions that govern their nucleosynthesis. In addition, we present web-based tools that allow any interested researcher to explore reaction-rate sensitivities in the alpha-rich freezeout and thereby make a case for experiments on nuclear reactions important for other observables (yet to be identified) from this process. We hope that this work can serve as a template for future work (by ourselves or others) on nuclear reactions important in other nucleosynthesis processes.

This paper begins with an introduction to the alpha-rich freezeout and a description of our freezeout calculations and the attendant reaction-rate sensitivity studies in §II. In §III we introduce two web sites accessible from the main page <http://photon.phys.clemson.edu/gjordan/nucleo/>. The first website displays data from the sensitivity calculation performed on our alpha-rich freezeout model in order to identify nuclear reactions that are important in the production of nuclei identified as astrophysical observables. With a particular isotope in mind, one may then use the web site to view the effect of different reaction rates on the yield of that isotope. The second website can be used to calculate the effects of a varied reaction rate on nucleosynthesis yields under conditions that differ from the conditions used in our sensitivity survey. Control over several of the parameters in the explosive model is given to the user so that the effect of a particular reaction rate on the network yields can be explored over a wide variety of conditions, thereby allowing the user to strengthen his case for measuring a particular reaction. Finally, due to their significance as astrophysical observables, several isotopes from the iron-group nuclei are examined §IV.

II. THE CALCULATIONS

Many processes contribute to the production of new nuclei in core-collapse supernovae, but one of the most important for astronomy is the alpha-rich freezeout from equilibrium. During the core collapse of a dying massive star, a shock wave develops as matter falls supersonically onto the collapsed stellar core. The shock, aided by a push from neutrinos

from the cooling nascent neutron star, expands out into, heats, and expels the overlying stellar matter. In the initial heating of the innermost regions of the ejecta, post-shock temperatures are sufficiently high that nuclei are broken down into nucleons and α particles. As the material subsequently expands and cools, the nucleons and α particles reassemble to form heavy nuclei. Because of the fast expansion of the matter, however, not all alpha particles reassemble, and, as a result, the final abundances freeze out with a significant number α particles remaining, hence the name alpha-rich freezeout. A number of significant astronomical observables are produced in this process including ^{44}Ti , ^{56}Co , and ^{57}Co .

In order to explore the sensitivity of alpha-rich freezeout yields to variations in reaction rates, we utilized the Clemson nucleosynthesis code [3], which we have updated to employ the NACRE [4] and NON-SMOKER [5] rate compilations. The network used (see [2]) includes 376 species from neutrons up to $Z = 35$ (Bromine) and 2,125 reactions among them.

We began the survey with calculations using reaction rates from the compilations. Guided by detailed models of such astrophysical settings (e. g., [6]), we chose an initial temperature of $T_9 = T/10^9\text{K} = 5.5$ and initial density $\rho_0 = 10^7 \text{ g/cm}^3$ in all calculations. The matter was taken to expand exponentially so that the density evolved with time t as $\rho(t) = \rho_0 \exp(-t/\tau_{ex})$, where the density e-folding timescale $\tau_{ex} = 446 \text{ s}/\sqrt{\rho_0} = 0.141 \text{ s}$. We assume the relation $\rho \propto T^3$ (radiation-dominated expansion), and took three possible values of the neutron excess η , viz., 0, 0.002, and 0.006. Since we considered the appropriate model for alpha-rich freezeout to be the passage of a shock wave through ^{28}Si -dominated matter, the initial composition was ^{28}Si with enough ^{29}Si to give the appropriate value of η .

Upon completion of these reference calculations, we explored the significance of a particular reaction by multiplying the reference value for its rate by a factor of ten, and repeating the calculation with the same expansion parameters as in the reference calculations. We emphasize that, with this procedure, we uniformly increase the rate at all temperatures by a factor of ten. The corresponding reverse reaction rate is also increased by the same factor at all temperatures. This is required by detailed balance to ensure the material reaches the appropriate equilibrium at high enough temperature and density. We repeated this procedure for all 2,125 reactions and all values of initial η 's. We also repeated this sequence with a multiplicative factor 0.1 on each of the reactions. The total number of alpha-rich freezeout calculations performed was (number of reactions) \times (number of different values of η) \times (number of multiplicative factors) + (number of reference calculations)

$$= 2,125 \times 3 \times 2 + 3 = 12,753.$$

The effect of modifying a particular reaction can be determined from the ratio of the modified yield of a particular species with the reference yield. Clearly with 2,125 reactions and 376 species, there are many combinations to consider. Rather than present several large tables, we have opted to construct interactive web-based applications to display the results.

III. INTERNET APPLICATIONS

In this section we introduce two web-based applications. Since the web sites have complete online help files, detailed instructions are not given here. We will simply introduce the web sites and some of their relevant features, along with instructions on how to reproduce the tables appearing in the following sections.

A. Network Sensitivity Data Display

The Sensitivity Data Display website is designed to examine the results of varying the reaction rates involving a selected isotope. Upon loading the page, the user selects from one of six data sets. The data sets are specified by η and by whether the reaction rates are increased or decreased (by a factor of 10 in each case). Next, the user can generate lists sorted by increasing or decreasing modified-to-standard ratios for a selected isotope. An isotope (the chosen observable) is selected by entering its atomic number and mass number in the appropriate fields. A β -decay option is also available which permits the user to evolve the abundances to arbitrarily later times upon cessation of the alpha-rich freezeout process. (The numerical technique used to construct the exact solutions to the coupled differential equations governing the β -decay of the abundances is described in the Appendix).

The data in Tables V, VI, and VII of §IV were collected using this web site. To reconstruct Table VII, for example, the user selects the data set corresponding to $\eta=0.006$ and a multiplicative factor of 0.1. For ^{55}Fe , 26 is entered as the Z value and 55 for the A value. We target an observation of the ^{55}Fe abundance made 2 years after the explosion, and so the user selects the β -decay box and enters an evolution time of 2 years into the time field.

In order to display only the reactions that change the ^{55}Fe yield by more than 20%, the ratio cut-off parameter is set to 0.20. The “Descending List” button is then clicked to

generate the ratio list for ^{55}Fe . The first table generated produced gives the mass fractions of all $A = 55$ species in the network at the end of the $\eta = 0.006$ reference alpha-rich freezeout calculation together with their beta-decay or electron-capture lifetimes. Isotopes highlighted in black are stable while those in pink are unstable against β^+ or electron capture. Isotopes highlighted in blue are subject to β^- -decay while green denotes instability via both channels.

In the second table, the column on the far right of the output contains the modified-to-standard ratios after an interval of two years. The reactions which, when their rate is decreased by a factor of ten, result in a minimum increase in the yield of ^{55}Fe of 20% are entered in the table along with the respective ratios. Similarly, those reactions which, when their rate is decreased by a factor of ten, result in at least a 20% decrease in the ^{55}Fe yield were also entered in the table along with their ratios. The process was then repeated with a rate factor of 10 and η of 0.006. The data for Tables Vi and VI were created in a similar manner, but for the isotopes ^{57}Co and ^{59}Ni .

Other options on the web site include (a) a table of the isotopes used in network calculations, (b) a list of reaction rates included in the calculations and (c) a tool for the user to plot or make a table of the standard reaction rates used in the calculations. The user can use the reaction number from the reaction list and then input that reaction into the reaction-rate engine to obtain either a plot or table of the rate as a function of temperature. (Note that the rate we present may include a stellar enhancement factor to correct for the possibility of excited states in the target nucleus. The user must account for this factor when comparing his rate with the one we used.) Other links on the page are to various related topics in the help file and to the NACRE and NON-SMOKER rate compilation web sites.

B. Explosive Nuclear Burning

The Explosive Nuclear Burning web site simulates parameterized explosive nuclear burning over the web using the same reaction network as described above. Among the variable parameters are T_9 (initial temperature in 10^9 K), ρ (initial density in g/cm^3), τ_{ex} (the expansion time scale of the explosion), and the initial mass fraction of each species. The user can also alter any reaction rate in the network by a multiplicative factor as was done in § II.

The data output from the web site are the final mass fractions from the calculation. If a reaction rate is modified, the web site performs two calculations, one with the modified

reaction rate, and one with the standard reaction rates for comparison. The data output in this case are the final mass fractions from both calculations along with their modified-to-standard ratios. The web site offers several options for further analysis, including a β -decay option to evolve the final mass fractions in the output.

This web site was used to produce the data from Tables I, II, III, and IV. To reconstruct these tables, the user performs the following steps. First, the user selects the default parameters, which correspond to an alpha-rich freezeout of silicon-dominated matter with an η of 0.006 (the parameters the sensitivity calculations in § II). When the calculation is executed, the appropriate mass fractions are inserted into the “t = 0 years” column of the Table. The β -decay box is then selected from the “Final Mass Fraction Data List Controls” table in the left hand frame and a time of 2 years entered. The “Create List” button is then clicked. The web site returns a table with the value of all of the final mass fractions after 2 years. The final mass fractions should agree with those in Tables I, II, III, and IV.

The data for Table VIII was also generated with this web site. To reconstruct this table, the user performs the following steps. First, the web site is reloaded into the browser. Then the “Edit” button in the “Reaction Rates” row of the “Parameter Controls” table in the left hand frame is clicked. This brings up an interface that allows the user to select a reaction rate to modify based on the type of reaction preferred. Since the reaction of interest in Table VIII is $^{55}\text{Co}(p, \gamma)^{56}\text{Ni}$ (a two nuclear species to one nuclear species reaction), the radio button at the bottom of the table entitled “ $i + j \rightarrow k$ ” is clicked. Starting at the left hand side of this table, the constituents of the reaction are chosen field by field. When all of the fields in the table are selected, the “Save Changes” button at top (or bottom) of the page is clicked. The user is then prompted to input a reaction rate multiplier. A value of 100 is entered and the “Save Changes” button clicked. The web site then presents a summary of the changes and the calculation is begun by clicking the “Run Nucleosynthesis Code” button. The outputted data are then evolved for two years as above and the appropriate modified-to-standard ratio is entered into Table VIII. The web site is then reloaded and the same procedure is carried out except 0.01 is entered as the multiplicative factor on the $^{55}\text{Co}(p, \gamma)^{56}\text{Ni}$ reaction rate. These steps should reproduce the data in Table VIII.

This web site has many other useful tools that are not described above but are documented in the on-line help files. As shown, this web site allows the user to examine the effects of a reaction on nucleosynthesis yields under a wide variety of circumstances. Our hope is that

this easily accessible data will provide additional insight into the effects that uncertainties in reaction rates have on the yields of the alpha-rich freezeout and other nucleosynthesis processes.

IV. NUCLEAR REACTIONS GOVERNING THE SYNTHESIS OF IRON-GROUP OBSERVABLES

In this section, we present some results of our calculations drawn from the web sites described in § III. For brevity we limit the discussion to the $\eta = 0.006$ calculations. The purpose is to illustrate how one may identify relevant observables and identify their governing reactions using the web sites.

At least three types of isotopic observables are relevant for stellar nucleosynthesis:

1. The bulk yields are important for understanding galactic chemical evolution and solar system abundances.
2. Radioactive species such as ^{26}Al and ^{44}Ti can be observed from space telescopes, and consequently provide important constraints on their production sites.
3. Isotopic abundances in presolar meteoritic grains carry important information about the nucleosynthesis environments in which their isotopes formed and the astrophysical settings in which the dust grains condensed (e. g., [7, 8]).

In the subsections to follow, we present several isotopes from the iron-group nuclei for which we used the web-based applications in § III to obtain data. These four isotopes are directly or indirectly linked to all three types of observables listed above. We have chosen to analyze ^{57}Co and ^{56}Co because of their prominent role as γ -ray observables and ^{59}Ni and ^{55}Fe for their potential as future X-ray observables. In addition, the abundances of the daughter isotopes of all four of these species may eventually be measured in presolar grains. We do not analyze ^{44}Ti , a key alpha-rich freezeout observable, because this has been done previously [2].

For each species, we list any reaction rate that produces at least a 20% increase or decrease in the alpha-rich freezeout yield due to a factor of 10 change in the reaction rate (except for ^{57}Co as explained below). Since we primarily consider the γ -ray or X-ray observations of

these species, we chose a time of analysis 2 years after the freezeout. By this time, overlying supernova should have become transparent to these radiations. Often, several years pass, if not thousands, before data from astronomical observables can be collected. It is, therefore, up to the user to make his own analyses using appropriately chosen times in the web tools described in §III. For each observable considered, we list the important reactions, and for two particularly interesting reactions we explore in some detail the reason for their effect on the chosen observable.

A. ^{56}Co

This species is produced primarily as the radioactive parent ^{56}Ni ($\tau_{1/2} = 6.075$ days) which decays through ^{56}Co ($\tau_{1/2} = 77.2$ days) to ^{56}Fe (see Table I). The overlying supernova largely obscures γ -rays from the decay of ^{56}Ni , but the 2.598 Mev γ -rays (for example) from the ^{56}Co can escape and be detected [9], making the latter species a valuable alpha-rich freezeout observable[21]. The γ -rays from ^{56}Co decay can be used to determine the total yield of the parent (^{56}Ni) as well as the opacities of the outer envelope of the supernova (for a review of γ -ray observables see [10]).

From the web sites one finds that the abundance of ^{56}Co after two years is dependent on the yield of ^{56}Ni from the supernova. We find that the yield of ^{56}Ni immediately after the $\eta = 0.006$ alpha-rich freezeout is quite insensitive to factor-of-ten changes in the reaction rates. The largest effect was due to changes in the triple- α reaction which produced about a 6% change in the yield. This 6% change propagates as a 6% change in the yield of ^{56}Co after the decay of ^{56}Ni . These are not significant changes and we conclude that the calculated yields of ^{56}Ni (and thus the yields of ^{56}Co) are quite robust against any reaction rate uncertainties. This result is expected since the production of ^{56}Ni is dominated by the equilibrium phase of the expansion in which the abundances are set by binding energies and nuclear partition functions (not by individual reaction rates).

B. ^{57}Co

A second important isotope is ^{57}Co . This isotope is similar to ^{56}Co in that its stable daughter ^{57}Fe owes a significant portion of its synthesis to alpha-rich freezeouts. From

Table II we see that ^{57}Co is primarily produced as the parent isotope ^{57}Ni . Gamma-rays from the decay of ^{57}Co are observable with space detectors, and they also power the supernova light curve at somewhat later times than ^{56}Co [11]. As shown, factors that affect the yield of ^{57}Ni thus have an effect on the yield of ^{57}Co .

The web sites show that the yield of ^{57}Ni immediately after the alpha-rich freezeout is (like ^{56}Ni) largely insensitive to the value of any particular reaction rate because both are primarily equilibrium products. The reaction with the most significant effect (for $\eta = 0.006$) is $^{57}\text{Ni}(n,p)^{57}\text{Co}$. We have chosen to list this reaction even though it does not produce more than a 20% change because of the importance of ^{57}Co as an observable. From Table V we see that this reaction produces at most a 17.7% change in the yield of ^{57}Ni for a factor of ten change in the rate. The primary reaction rate governing the yield of ^{57}Co for $\eta = 0.006$ is $^{57}\text{Ni}(n,p)^{57}\text{Co}$ and a factor of a few uncertainty in the reaction rate results in a several percent uncertainty in the observable.

The reason $^{57}\text{Ni}(n,p)^{57}\text{Co}$ has an effect on the yield of ^{57}Ni (and thus the yield of ^{57}Co) is that it governs when ^{57}Ni falls out of quasi-statistical equilibrium (QSE—see, for example, [12]). As shown in figure 1, the ^{57}Ni abundance diverges from nuclear statistical equilibrium (NSE) early but remains in line with QSE expectations until it freezes out below $T_9 \approx 3.5$. The QSE favors ^{57}Ni early, but as the material cools below $T_9 \approx 4.3$, the QSE abundances shift to higher-mass nuclei; thus, the longer ^{57}Ni remains in QSE, the lower its final abundance. ^{57}Ni falls out of QSE when the $^{57}\text{Ni}(n,p)^{57}\text{Co}$ reaction becomes too slow, which means that increasing the rate for this reaction causes ^{57}Ni to remain in QSE longer and to have a lower final abundance. Decreasing the rate means ^{57}Ni falls out of QSE earlier and retains more of its originally high QSE abundance.

C. ^{59}Ni

Both ^{59}Ni and ^{55}Fe have been chosen because they hold promise as detectable radioactive X-ray sources (for a prospectus see [13]). In the decay of these isotopes by electron capture, a K-shell vacancy occurs which is often filled by an electron previously occupying a higher-level bound state. The energy loss from this event is carried away as an X-ray which, if detected, would not only provide data complementary to γ -ray observations, but also shed light on the production of radioactive isotopes that emit no γ -rays.

The observable ^{59}Ni , because of its 75,000 y half-life, should produce a significant diffuse emission from the interstellar medium similar to that observed from interstellar ^{26}Al . It may also be detectable in close, individual supernova remnants [14]. From Table III we see that the majority of ^{59}Ni is produced in the alpha-rich freezeout as ^{59}Cu ; thus, factors that affect the production of ^{59}Cu ultimately affect the production of the observable ^{59}Ni . From the web sites it is evident that there are several reactions which, when changed by an order of magnitude, have a moderate effect on the production of ^{59}Cu (see Table VI). The most influential of these is the $^{59}\text{Cu}(p,\gamma)^{60}\text{Zn}$ reaction. A factor of 10 decrease in this reaction rate produces about a 50% increase in the yield, while a factor of 10 increase in the reaction rate drops the yield of ^{59}Cu by about 30%. These are modestly significant changes and show that ^{59}Ni is sensitive to specific reactions in the alpha-rich freezeout.

D. ^{55}Fe

Unlike ^{59}Ni , ^{55}Fe has a relatively short half life ($\tau_{1/2} = 2.73$ yrs), making it only detectable in very young supernovae (supernova 1987A remains a good target for detecting ^{55}Fe [13]). Since the detection of ^{55}Fe could become available at very early times after the explosion (assuming the ejecta is transparent to X-rays), its detection should give information on small-scale structure formation in the ejecta. Further, it may help elucidate the velocity structure of the core and the velocity structure of ^{55}Fe [14].

As can be seen from Table IV, ^{55}Fe is predominantly produced as ^{55}Co . The production of ^{55}Co in the alpha-rich freezeout with $\eta = 0.006$ is most sensitive to the triple- α reaction and the $^{55}\text{Co}(p,\gamma)^{56}\text{Ni}$ reaction (Table VII). The triple- α reaction has about a factor of two effect on the yield when a factor of 10 change in the triple- α rate is made. The largest effect on the yield is seen in the dependence of the ^{55}Co abundance on the $^{55}\text{Co}(p,\gamma)^{56}\text{Ni}$ reaction. A factor of 10 decrease in this reaction rate increases the yield of ^{55}Co by 526% while an increase in the reaction rate reduces the yield by almost 80%.

The reason for the sensitivity of ^{55}Co to the $^{55}\text{Co}(p,\gamma)^{56}\text{Ni}$ reaction rate is similar to that of the sensitivity of ^{57}Ni to the $^{57}\text{Ni}(n,p)^{57}\text{Co}$ reaction rate, but the effect is much larger. The ^{55}Co remains in (p, γ)-(γ ,p) equilibrium with abundant ^{56}Ni until T_9 drops below 3.0. As the temperature drops, the equilibrium shifts abundance from ^{55}Co to higher-mass nuclei (particularly ^{56}Ni). Increasing the $^{55}\text{Co}(p,\gamma)^{56}\text{Ni}$ reaction rate causes this abundance shift to

persist longer, which in turn leads to a lower final ^{55}Co yield. A lower value for the reaction rate leads to an earlier freezeout from QSE and a higher final ^{55}Co yield. From this we see that ^{55}Co , and thus ^{55}Fe (the relevant observable), are very sensitive to the $^{55}\text{Co}(p, \gamma)^{56}\text{Ni}$ reaction rate.

V. CONCLUSION

The above described web sites are intended to be a starting point for identifying those nuclear reactions that govern the production of astrophysical observables from the alpha-rich freezeout. It is our hope that these web sites will help motivate future measurements of these key reactions, especially as new observables from the alpha-rich freezeout are identified.

While we identified and analyzed four key observables from the alpha-rich freezeout, we expect new ideas or emphases in astrophysics to make new observables available. For example, as models of Galactic chemical evolution become increasingly refined, better yields from massive stars will become necessary. This means that any isotope that owes a significant portion of its solar system abundance to the alpha-rich freezeout, such as ^{40}Ca , ^{48}Ti , $^{52,53}\text{Cr}$ and the ones discussed above, will become an observable. Similarly, new technologies may also open new possibilities for observing isotopes. As a possible example, ^{44}Ca excesses found in presolar supernova silicon carbide (SiC) X grains arose from condensation of live ^{44}Ti [15]. One speculation is that much of this excess radiogenic ^{44}Ca may be concentrated in small titanium carbide (TiC) subgrains within the larger SiC X grains. Such TiC subgrains are known to exist in mainstream SiC grains that condensed in outflows from low-mass stars [16, 17]; however, in two SiC X grains studied so far, there is no direct evidence for the presence of such TiC subgrains[18], though the search continues. If such subgrains do exist, they are likely to be dominantly comprised of alpha-rich freezeout material. If the new generation of secondary-ion mass spectrometers are able to measure the isotopic abundances in the subgrains, then the alpha-rich freezeout abundances of all titanium and carbon isotopes, as well as the isotopes of any element that might condense in TiC, would become observables. Those new observables will open up new governing reactions requiring experimental study.

We view the web sites presented here as a first step for similar, future work on other nucleosynthesis processes. The goal in those future efforts, as in the present work, will be

to help identify nuclear reactions that govern the nucleosynthesis of astronomical observables. As always, however, the challenge remains not only to identify nuclear reactions that govern the synthesis of those observables, but also to identify the key astronomical observables themselves. Only by maintaining a healthy dialogue among astronomers, astrophysical modelers, and nuclear experimentalists can we face that challenge and advance the science of nuclear astrophysics.

Acknowledgments

This research was supported by NASA grant NAG5-4703, NSF grant AST-9819877, and a DOE SciDAC grant. The authors acknowledge helpful discussions with D. D. Clayton, M. D. Leising and P. Mohr.

-
- [1] A. A. Sonzogni, K. E. Rehm, I. Ahmad, F. Borasi, D. L. Bowers, F. Brumwell, J. Caggiano, C. N. Davids, J. P. Greene, B. Harss, et al., *Physical Review Letters* **84**, 1651 (2000).
 - [2] L. S. The, D. D. Clayton, L. Jin, and B. S. Meyer, *Astrophys. J.* **504**, 500 (1998).
 - [3] B. S. Meyer, *Astrophys. J. Lett.* **449**, L55 (1995).
 - [4] C. Angulo, M. Arnould, M. Rayet, P. Descouvemont, D. Baye, C. Leclercq-Willain, A. Coc, S. Barhoumi, P. Aguer, C. Rolfs, et al., *Nuclear Physics A* **656**, 3 (1999).
 - [5] T. Rauscher and F. Thielemann, *Atomic Data and Nuclear Data Tables* **75**, 1 (2000).
 - [6] F. Thielemann, K. Nomoto, and M. Hashimoto, *Astrophys. J.* **460**, 408 (1996).
 - [7] A. M. Davis, R. Gallino, M. Lugaro, C. E. Tripa, M. R. Savina, M. J. Pellin, and R. S. Lewis, in *Lunar and Planetary Institute Conference* (2002), vol. 33.
 - [8] D. D. Clayton, B. S. Meyer, L.-S. The, and M. F. El Eid, *Astrophys. J. Lett.* **578**, L83 (2002).
 - [9] M. D. Leising and G. H. Share, *Astrophys. J.* **357**, 638 (1990).
 - [10] R. Diehl and F. X. Timmes, *Pub. Astron. Soc. Pac.* **110**, 637 (1998).
 - [11] M. D. Leising, W. N. Johnson, J. D. Kurfess, D. D. Clayton, D. A. Grabelsky, G. V. Jung, R. L. Kinzer, W. R. Purcell, M. S. Strickman, L.-S. The, et al., *Astrophys. J.* **450**, 805 (1995).
 - [12] B. S. Meyer, T. D. Krishnan, and D. D. Clayton, *Astrophys. J.* **498**, 808 (1998).
 - [13] M. D. Leising, *Astrophys. J.* **563**, 185 (2001).

- [14] M. Leising, *New Astronomy Review* **46**, 529 (2002).
- [15] L. R. Nittler, S. Amari, E. Zinner, S. E. Woosley, and R. S. Lewis, *Astrophys. J. Lett.* **462**, L31 (1996).
- [16] T. J. Bernatowicz, S. Amari, and R. S. Lewis, *LPI Contributions* **781**, 1 (1992).
- [17] P. Hoppe, R. Strebel, P. Eberhardt, S. Amari, and R. S. Lewis, *Meteoritics and Planetary Science* **35**, 1157 (2000).
- [18] A. Besmehn and P. Hoppe, in *Lunar and Planetary Institute Conference Abstracts* (2002), vol. 33.
- [19] F. X. Timmes, S. E. Woosley, and T. A. Weaver, *Astrophys. J. Suppl.* **98**, 617 (1995).
- [20] D. S. Watkins, *Fundamentals of Matrix Computations* (John Wiley, New York, 1991).
- [21] It should be clear that the bulk yield of ^{56}Fe from the alpha-rich freezeout may also be considered an observable since approximately half of the ^{56}Fe in the solar system was produced by alpha-rich freezeouts in core-collapse supernovae (e. g., [19]). Accurate alpha-rich freezeout yield predictions are required for Galactic chemical evolution models to reproduced the solar system's supply of ^{56}Fe .

APPENDIX: ANALYSIS OF THE β -DECAY ALGORITHM

We now draw attention to the algorithm used by the Sensitivity Data Display and the Explosive Nucleosynthesis web-sites to compute alpha-rich freezeout yields at a specified point in time. Traditional approaches rely on Runge-Kutta or implicit Euler techniques to integrate the coupled differential equations (preferably with adaptive timestep adjustments). However, we have sought a rapid, but exact solution. To do this, we exploit the elementary matrix solution to the system of linear coupled DEs that utilizes eigenvalues and eigenvectors. For any matrix equation of the form

$$\dot{\mathbf{x}} = \mathbf{A}\mathbf{x} \tag{A.1}$$

$$\mathbf{x}(0) = \mathbf{b} \tag{A.2}$$

the solution at all later times is given by:

$$\mathbf{x}(t) = \sum c_k(\Phi_k e^{\omega_k t}), \tag{A.3}$$

where Φ_k are the eigenvectors and ω_k the corresponding eigenvalues of the matrix \mathbf{A} (constructed from β -decay rates and the application of mass conservation) which remain constant during the evolution. The coefficients c_k of the linear combination are the elements of the product $\mathbf{T}^{-1}\mathbf{b}$ (where \mathbf{T} is the matrix of eigenvectors of \mathbf{A} ordered strictly according to the index “ k ”)

The technical challenge here is that \mathbf{A} is singular and thus reduction to upper Hessenberg form (the practical method of computing the spectrum of a large asymmetric system) using QR Factorization fails. We may circumvent this difficulty by employing very small perturbations to the rates and thus disturbing the rate matrix away from singularity, as is the norm for practical Numerical Linear Algebra applications in most fields of engineering. However, we must be cognizant of the fact that a theorem of Watkins [20] requires the eigenvalues to be reasonably separated for the system to be insensitive to perturbations. Unfortunately for the full 376×376 matrix, the observed degeneracies are quite severe.

On closer inspection, however, it is realized that the cause of the degeneracies is quite simple: the matrix is composed of several non-communicating blocks. Since only β -decays are considered, the vector space decomposes into the *direct sum* of these blocks, each corresponding to a particular mass number. Blocks comprised of isotopes from different mass numbers cannot traffic with each other since we exclude other kinds of nuclear reactions. Several of these component submatrices are very similar in their spectra, and therefore the full space suffers from many closely spaced eigenvalues.

The solution, however, is now obvious—we merely compute the spectrum of each block, confident in the knowledge that the isotopes within a particular block are not affected by those in any other. The complete state vector of the abundances at any given time is then a simple concatenation of the state vectors from the subspaces. Watkins’ theorem is now observed to hold for each block (though the blocks themselves are singular as the full matrix was before) and abundances are output within seconds.

Obviously, the next step is to extend the perturbation technique to matrices which *cannot* be decomposed into non-communicating subspaces (blocks). Weakly coupled blocks may lend themselves to similar perturbation analyses. Unfortunately Watkins’ theorem does not predict error bounds and the most we can do at this stage is carry out some rough numerical experiments to check the sensitivity of the system to small random perturbations. In our trials we found the effects to be negligible. Propagation of the perturbations caused fluctu-

ations on the order of 10^{-15} in the most ill-conditioned blocks. Abundances of order 10^{-15} or less are quite small and for any practical purpose such small abundances are nonexistent. We conclude that the system was very robust to the small kicks we gave it.

We hope to incorporate the latest techniques in spectral computations on large asymmetric systems as they become available, since nucleosynthesis would be an exciting test-bed for these tools from the frontlines of research in Numerical Linear Algebra. In the interim, perturbation allows us to practically carry out an important calculation in seconds which would otherwise have been impossible if we were to insist on a spectral solution.

TABLE I: Mass Fractions for A=56 with $\eta = 0.006$

Isotope	t = 0 years	t = 2 years
^{56}Ni	0.767	0
^{56}Co	3.356×10^{-6}	1.190×10^{-3}
^{56}Fe	5.161×10^{-12}	0.766

TABLE II: Mass Fractions for A=57 with $\eta = 0.006$

Isotope	t = 0 years	t = 2 years
^{57}Cu	0	0
^{57}Ni	3.967×10^{-2}	0
^{57}Co	6.735×10^{-7}	6.197×10^{-3}
^{57}Fe	3.429×10^{-14}	3.348×10^{-2}

TABLE III: Mass Fractions for A=59 with $\eta = 0.006$

Isotope	t = 0 years	t = 2 years
^{59}Ga	0	0
^{59}Zn	6.260×10^{-14}	0
^{59}Cu	1.887×10^{-3}	0
^{59}Ni	4.065×10^{-5}	1.928×10^{-3}
^{59}Co	3.682×10^{-13}	3.562×10^{-8}

TABLE IV: Mass Fractions for A=55 with $\eta = 0.006$

Isotope	t = 0 years	t = 2 years
^{55}Ni	3.306×10^{-10}	0
^{55}Co	1.013×10^{-5}	0
^{55}Fe	3.393×10^{-10}	6.058×10^{-6}
^{55}Mn	0	4.072×10^{-6}

TABLE V: Data from the $\eta = 0.006$ network survey for ^{57}Co

Reaction	Reaction Rate $\times 0.1$	Reaction Rate $\times 10.0$
$^{57}\text{Ni}(\text{n,p})^{57}\text{Co}$	1.177	0.876

TABLE VI: Data from the $\eta = 0.006$ network survey for ^{59}Ni

Reaction	Reaction Rate $\times 0.1$	Reaction Rate $\times 10.0$
$^{59}\text{Cu}(\text{p},\gamma)^{60}\text{Zn}$	1.556	0.615
$2\alpha(\alpha)^{12}\text{C}$	1.324	0.731
$^{59}\text{Cu}(\text{p},\alpha)^{56}\text{Ni}$	0.848	1.444

TABLE VII: Data from the $\eta = 0.006$ network survey for ^{55}Fe

Reaction	Reaction Rate $\times 0.1$	Reaction Rate $\times 10.0$
$^{55}\text{Co}(\text{p},\gamma)^{56}\text{Ni}$	5.258	0.232
$^{59}\text{Cu}(\text{p},\alpha)^{56}\text{Ni}$	1.170	0.738
$^{59}\text{Cu}(\text{p},\gamma)^{60}\text{Zn}$	0.690	1.133
$2\alpha(\alpha)^{12}\text{C}$	0.561	1.887

TABLE VIII: Data from web based Explosive Silicon Burning with $\eta = 0.006$ for ^{55}Fe

Reaction	Reaction Rate $\times 0.01$	Reaction Rate $\times 100.0$
$^{55}\text{Co}(\text{p},\gamma)^{56}\text{Ni}$	34.544	5.469×10^{-2}

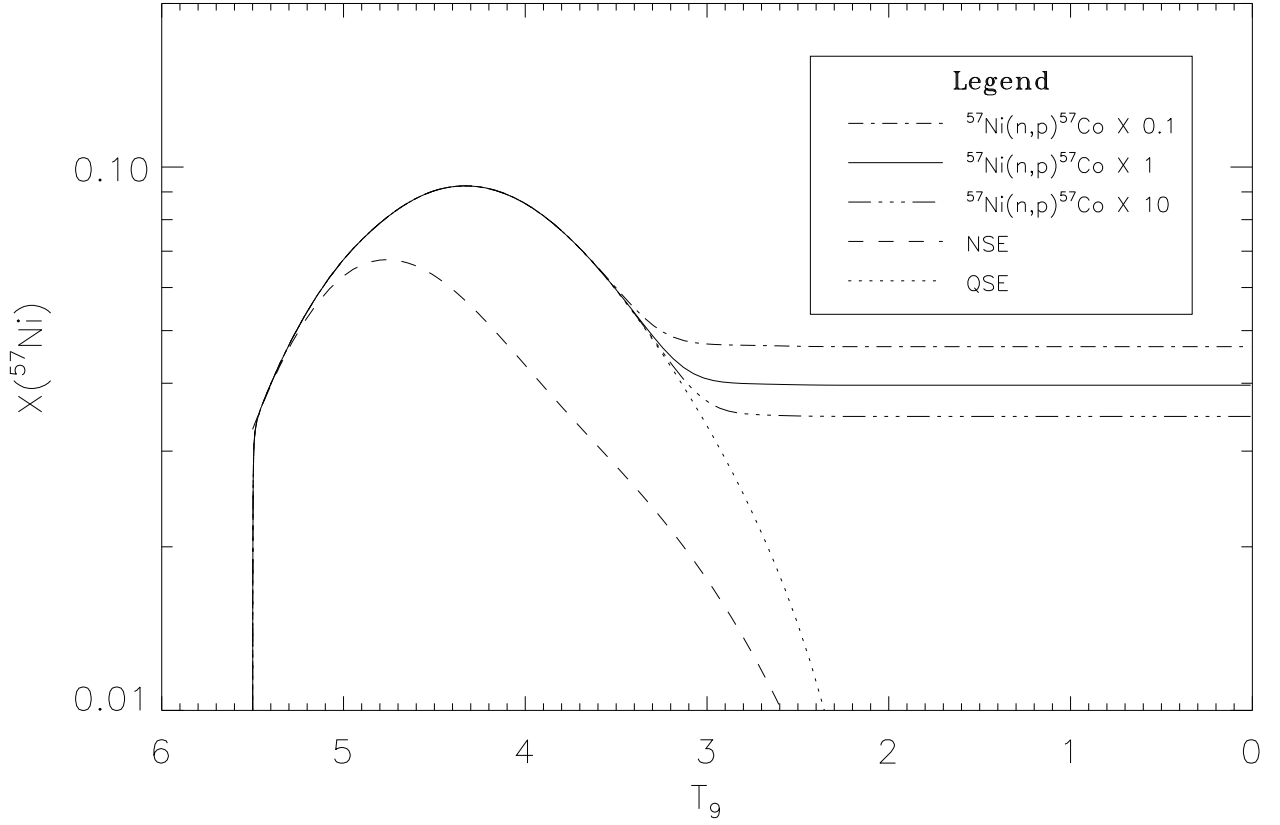


FIG. 1: Mass fraction of ^{57}Ni versus T_9 for different values of the reaction rate $^{57}\text{Ni}(n,p)^{57}\text{Co}$ and in NSE and QSE. The value of the reaction rate near $T_9 \approx 3.5$ governs when ^{57}Ni breaks out of QSE.

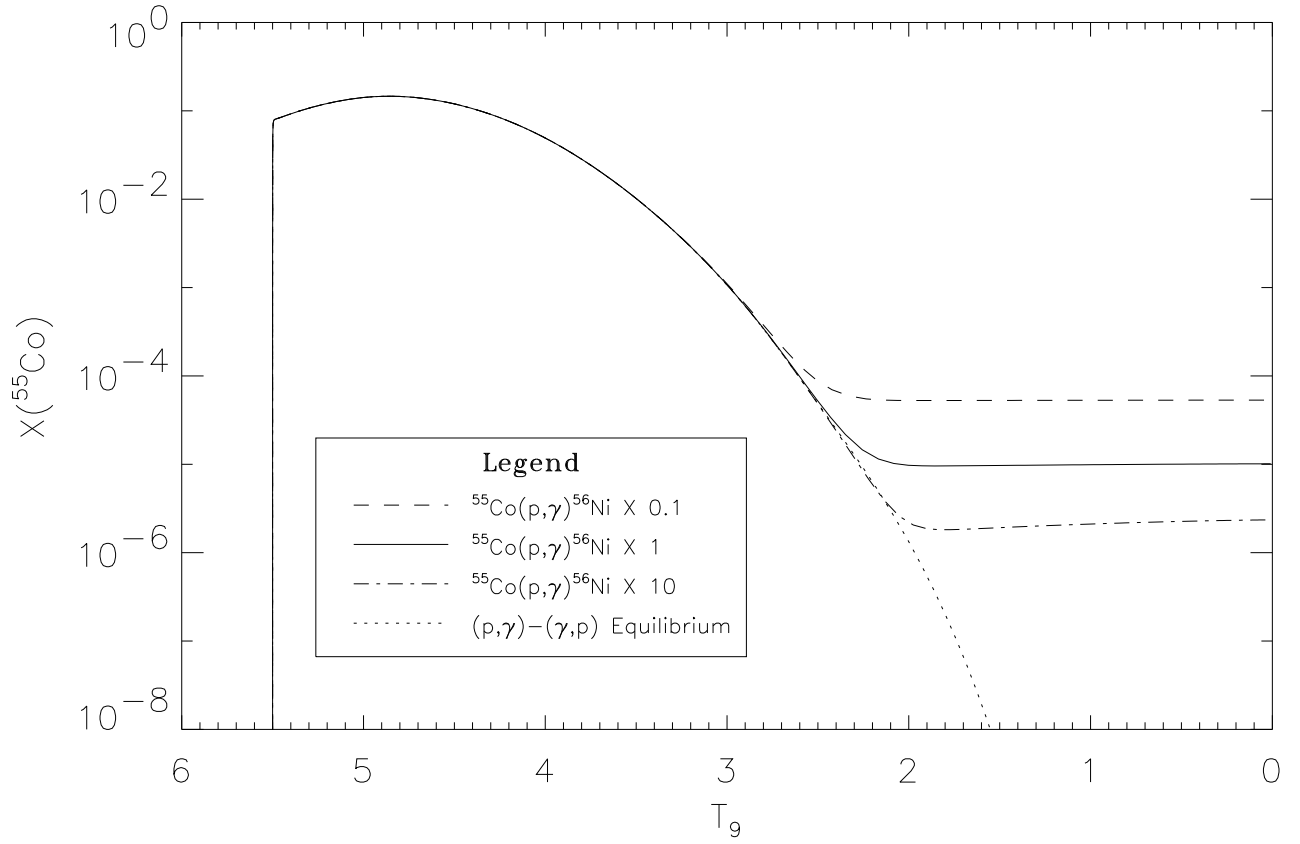


FIG. 2: Mass fraction of ${}^{55}\text{Co}$ versus T_9 for different values of the reaction rate ${}^{55}\text{Co}(p,\gamma){}^{56}\text{Ni}$ and in $(p,\gamma)-(\gamma,p)$ equilibrium. The value of the reaction rate near $T_9 \approx 2.5$ determines when ${}^{55}\text{Co}$ breaks out of $(p,\gamma)-(\gamma,p)$ equilibrium with ${}^{56}\text{Ni}$.